



## ORIGINAL RESEARCH PAPER

# Impact of advanced inverter functions on low-voltage power grids

Arjen Mentens<sup>1,2</sup> | Harold R. Chamorro<sup>2</sup> | Valéry Ann Jacobs<sup>3</sup> | David Topolánek<sup>4</sup> | Jiří Drápela<sup>4</sup> | Wilmar Martinez<sup>2</sup>

<sup>1</sup>Department of Engineering Technology (INDI), Vrije Universiteit Brussel, Brussels, Belgium

<sup>2</sup>Department of Electrical Engineering (ESAT), Katholieke Universiteit Leuven, Diepenbeek, Belgium

<sup>3</sup>Department of Electronics and Informatics (ETEC), Department of Applied Physics and Photonics (TONA), Rectorate, Vrije Universiteit Brussel, Brussels, Belgium

<sup>4</sup>Department of Electrical Power Engineering (UEEN), Brno University of Technology, Brno, Czech Republic

## Correspondence

Arjen Mentens, Department of Engineering Technology (INDI), Vrije Universiteit Brussel, Brussels, Belgium.  
Email: [Arjen.Mentens@vub.be](mailto:Arjen.Mentens@vub.be)

## Abstract

In today's power grid, a great number of inverter-based distributed energy resources (DERs) are connected and are mainly designed to supply power without considering the voltage and frequency deviations of the grid. Therefore, distribution system operators (DSOs) are challenged with an increase in grid events because of the random implementation of DERs. Voltage levels can vary beyond predefined limits at the point of connection and are currently not evaluated by DSOs. Summarized here is the development of a simulation model for evaluating the impact of support functions integrated in inverter-based DERs. The model aims to help grid operators simulate voltage and frequency events and study the impact of DERs to the grid with respect to different settings of integrated support functions. A model is developed in MATLAB/Simulink conforming to European standards and regulations. Grid dynamics can be evaluated by imitating voltage and frequency deviations. Support functions can be either adjusted according to the situation or turned off. Together with adjustable settings according to DSO request, this model offers flexibility and insight in the capabilities of DERs to solve voltage and frequency issues. Case studies show that the model corresponds to expected behaviour and can be used for further development.

## 1 | INTRODUCTION

The world is looking for opportunities to produce clean energy. While households account for over 27% of total energy demand, they (indirectly) account for an aggravation of global warming [1]. The Europe 2020 strategy includes targets for climate change and energy, and governments are promoting DERs with incentives [2, 3]. Worldwide, all (power-consuming) sectors contribute to around 38% of energy-related CO<sub>2</sub> emissions. Increasing and stimulating photovoltaic (PV) production can significantly reduce these emissions, as 1 kWh produced by PV emits as little as 15 g/kWh CO<sub>2</sub> compared with the global average of 475 g/kWh CO<sub>2</sub> [3]. While merely 3% of electricity is generated by PV, it avoids around 4.5% of power sector emissions. This is because of countries with high carbon electricity generation, such as China and India, installing a great amount of PV power [3–5].

In the past, power was only consumed but never supplied by households. And thus, for a long time, an on-load tap

changer (OLTC) was the only mechanism necessary to change local voltage levels. They rely on the fact that there is a uniform voltage drop across the power lines. Unfortunately, they no longer suffice. Due to the implementation of inverter-based DERs, mostly PV panels, the uniform voltage drop has become less common, and voltage levels can vary in both directions [6].

Situations even exist where PV panels are prohibited in parts of the grid [7]. Instead of prohibiting them, they can become part of the solution. Households are supplying an amount of power that can no longer be ignored. It was found that voltage deviations will not occur when the average penetration per household lies below 2.5 kW [8]. The study in [8] assumed a DER penetration level of 0%–11.25%, but penetration levels have risen to 22% [9, p. 13]. As a result, voltage deviations are occurring more frequently and with a higher amplitude but only impact the local grid [10]. Instead of reinforcing the grid, PV inverters can become an important part of grid support. For this reason,

This is an open access article under the terms of the Creative Commons Attribution-NonCommercial-NoDerivs License, which permits use and distribution in any medium, provided the original work is properly cited, the use is non-commercial and no modifications or adaptations are made.

© 2021 The Authors. *IET Energy Systems Integration* published by John Wiley & Sons Ltd on behalf of The Institution of Engineering and Technology and Tianjin University.

regulations have been implemented [11]. While PV is a clean alternative, it contributes only 2.9% of global electricity demand. This indicates that PV is not a comprehensive solution for abandoning polluting power-generating facilities. Ultimately, development of energy storage (electrical, thermal, hydrogen etc.) can play an important role in stimulating investments in renewable energy resources in general. The exponential growth of installed PV capacity is a first argument for how these installations could impact the distribution grid and also why they can and should be used as grid support. The worldwide cumulative installed capacity in 2008 was only 14.5 GW, while it exceeded 100 GW in 2012. However, in 2018, a fivefold level was already installed. Following this trend, it can be expected to reach 1 TW by 2022 [3].

Dynamic models with advanced functionalities of converter-based generation are crucial for understanding the behaviour of the grid under stressed circumstances [12, 13]. However, such functionalities bring various challenges associated with increased penetration of DERs and their grid interaction [14]. Smart inverters with voltage and frequency control abilities are valuable for DERs so they can contribute to the grid with support functions and ancillary services, such as reactive power control, fault ride-through, and harmonic compensation [15]. Many research papers have been published in recent years that discuss the voltage violation issues that emerge from the high penetration of inverter generation into the power systems [16]. For instance, a test system adapted from the medium-voltage distribution system in Ontario, Canada, is studied in [17], providing grid voltage support functionalities. An optimized control strategy to manage the reactive power resource generated by inverter-based generation is presented in [18] to improve the quality of the voltage distribution network and fulfil the latest technical requirements listed by distribution system operators (DSOs) in their grid codes. A case study dealing with long-term voltage instability in systems hosting active distribution networks is reported in [19]. The documented simulations show the effect of the restoration of distribution network voltage. A hybrid control strategy for supporting the voltage under fault conditions is presented in [20], demonstrating the simultaneous mitigation of voltage sags by injecting active and reactive power to ride through the perturbation and maintain grid voltage. Similarly, a voltage regulation scheme using a deadbeat controller that helps to mitigate fast voltage disturbances is presented in [21] that suppresses the transients in the system.

The authors in [22] propose a control scheme with a dynamic injection region for the inverter system that adapts to the set-points assigned by a centralized controller. Similarly, a control scheme that optimizes the real-time operation of active distribution networks while also considering the provision of voltage support as an ancillary service to the network requirements in Switzerland and investigate the operational modes of the DER inverters is presented in [23]. The static voltage control considering voltage-reactive power mode and dynamic and extensive voltage control with maximum utilization of DER capacity and system stability are studied in [24].

As the previous contributions discussed, various control strategies exist and are able to function well under different grid conditions. Also, it shows that applying a control strategy depends heavily on the chosen control method and parameters.

This paper discusses the development of a simulation model to provide grid operators with more insight regarding the effect of inverter-based DERs. Since the control parameters can have a great impact on the grid response, the proposed simulation model offers flexibility regarding parameter choice.

The rest of this paper is organized as follows. Section 2 describes the possible methods for providing grid support. Section 3 presents the model design and implementation in MATLAB and explains the importance of setting the correct time constants. The simulation results and discussions are presented in Section 4. Finally, the conclusions are given in Section 5.

## 2 | METHODS FOR PROVIDING GRID SUPPORT

### 2.1 | Active and reactive power compensation using inverters

As briefly mentioned above, the integration of DERs will result in an increased voltage at the point of connection (POC). Due to fluctuating injection of power (solar and wind power are not constant), the need for automated solutions is growing, which implies that (even automated) OLTCS are no longer sufficient. Using these DERs to compensate for low or high voltage is one of the most commonly discussed methods [6, 7, 25–30].

Figure 1 depicts an equivalent schematic of a power line. The resistance and inductance of the line correspond to the replacement R and L value.

The voltage in a certain point is given by

$$U = f(P, Q) \quad (1)$$

where

$$dU = \frac{\partial U}{\partial P} dP + \frac{\partial U}{\partial Q} dQ \quad (2)$$

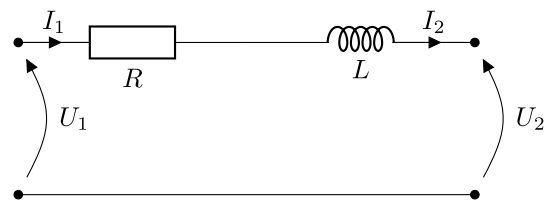


FIGURE 1 Power line with R and L components to indicate resistance and inductance values

and

$$\Delta U = U_1 - U_2 = R \cdot I_2 \cdot \cos\varphi_2 + X \cdot I_2 \cdot \sin\varphi_2 \quad (3)$$

with  $\varphi_2$  the phase shift between voltage  $U$  and current  $I_2$ . To rewrite Equation (4) as a function of  $P$  and  $Q$ ,

$$\Delta U = \frac{R \cdot P + X \cdot Q}{U_2} \quad (4)$$

Equation (4) indicates that the voltage drop  $\Delta U$  is related to the active and reactive power. It can also be seen that power lines with a high  $R/X$  ratio will experience more impact from a change in active power ( $P$ ) than a change in reactive power ( $Q$ ).

Three main types of inverter—a string inverter, a micro-inverter, and a central inverter—exist [31, 32]. A string inverter is based on solar panels connected in series. When one PV panel is shaded or malfunctions, the entire power output is limited by this one panel. A malfunctioning PV panel can be replaced, but shade caused by trees can often not be controlled by the owner. To overcome this, a micro-inverter can be installed instead. The PV panels are connected in parallel, and therefore only the shaded or malfunctioning panels are limited in output power. The difference with a central inverter is its size. Central inverters are mainly used in industrial installations with typical power ranges from 100 kW to 1 MW [32]. Due to its size, they are not considered here. The study in [31] also shows that microinverter systems present better performances at both shaded and not-shaded conditions. The main drawback of a microinverter is the higher cost. However, according to [33, p. 2885],

the string inverter appears to have a lower per-watt capital cost when just the inverter is considered. However, the inverter represents only about 15% of the entire PV system cost whereas the installation labour (...) cost accounts for 40%, depending on the system configuration and inverter technology. These factors have made it difficult to perform a comparative cost study.

The following functions are also known as advanced inverter functions and are discussed in [6, 34]. The set points at which these functions are deployed can differ according to the local requirements.

### 2.1.1 | Active power compensation

The possibility of the inverter to absorb  $P$  when there is overvoltage in the low-voltage (LV) grid is described as active power compensation. The inverter is set to start absorbing active power when a threshold voltage limit is met (e.g. at 3% overvoltage, the inverter shall start this compensation). First, it should be noted that this is only possible if a storage system is

present to absorb active power. If not, the inverter can reduce its  $P$  output, and if necessary, be disconnected from the grid. This will only happen in extreme situations. Also, being disconnected from the grid will cause a loss of income for the energy producer, so this should be avoided as much as possible. Second, this compensation is only available until the storage system is fully charged or until a threshold charge is reached.

### 2.1.2 | Reactive power compensation

In medium-voltage (MV) or LV grids where the reactance  $X$  is important,  $Q(U)$  compensation is used. In order to alleviate a voltage drop caused by a grid event, the inverter needs to provide a certain amount of  $Q$  to the grid [26, 35]. A deadband around the nominal voltage level is introduced to prevent the inverter from switching between absorbing or delivering  $Q$  in a short time span [36].

## 2.2 | Demand-side management results in a reduction of user comfort

Instead of limiting the output of an inverter, demand-side management (DSM) focuses on limiting power usage in case of high load and does the opposite in case of high injection. Washing machines, hot water buffers, and (in the future) electric vehicles may pose issues during peak hours [37]. The purpose is to postpone the usage of these appliances. In this manner, the load will be spread across a greater amount of time. The amount of postponed power is represented as flexibility [38, 39].

DSM is seen as an important method to help mitigate the effects of the increasing share of unpredictable renewable energy production, the increased electrical load due to fossil fuel powered equipment being replaced by electrical equipment, and the decreasing investments in directly controllable (fossil fuel) plants. To clarify the pros and cons of DSM, the necessities for a successful implementation and its contribution to blackouts are discussed.

### 2.2.1 | Necessities

Compared with using inverters, the requirements are more challenging. First, smart appliances are needed to control the power usage according to the voltage level at the POC, which was measured by a smart meter. These appliances consist of postponable appliances, such as dishwashers, washing machines and tumble dryers, and buffered appliances such as hot water buffers and electrical vehicles. Hot water buffers are considered to have the most influence on flexibility. Second, test families are equipped with a home energy management system. In a case study, one group was asked to alter their usage based on different energy tariffs during the day and the

other group was equipped with an Automated Home Energy Management System [38]. Appliances without smart capabilities were retrofitted with communication devices to ensure smart control. Smart appliances were turned on or off automatically, while basic comfort, such as always being able to take a hot shower, was still provided. Final, energy storage can be interesting for PV owners to promote self-consumption. It is not really seen as a necessity, as the price per kWh as well as the kWh per volume is still improving.

### 2.2.2 | Demand-side management as a solution for blackouts?

Considering that 18% of Flemish households heat their water using electricity (hot water buffers have the most impact as mentioned above), extrapolating this for the whole population of Belgium, delayed power usage would provide 207 MW of power. Taking into account the other appliances (washing machines, electric vehicles etc.) adds up to 267.9 MW. Comparing these values with the 725 MW strategic reserve that Belgian Transmission System Operator (TSO) Elia has to create, it can be assumed that, even with a participation grade of 100% of households with hot water buffers, the requirement will not be met [38, 40]. Nevertheless, DSM can become an important part of the solution.

In Belgium, most of the voltage support is provided by OLTCs. Once per year (or more, depending on the necessity) the tap stand of the transformer is changed to meet voltage limits. This is done manually, but more automated solutions are being implemented. To complement OLTC support, or even fully replace them, inverter-based DERs can be used. Both P and Q support functions can be implemented to alleviate voltage and frequency deviations.

Given the above, it is clear that additional grid support functions should be implemented in inverters to control voltage levels at the POC [11]. This should be extended from household DERs (e.g. PV panels) to inverter-based power plants. Before deployment of support functions, extensive testing needs to be performed in order to prevent errors and optimize effectiveness of implementation. The lack of comprehensible simulation models makes it more difficult to perform plausible tests [25].

## 3 | DESIGN AND IMPLEMENTATION USING MATLAB/SIMULINK

### 3.1 | Introduction

Testing and modelling will be performed in MATLAB/Simulink. Before its implementation, a basic LV grid model has to be developed. This model, as illustrated in Figure 2, consists of a voltage source, several loads that simulate household or industrial loads, and one or more DERs. The operator will be able to imitate grid events by switching loads on and off to

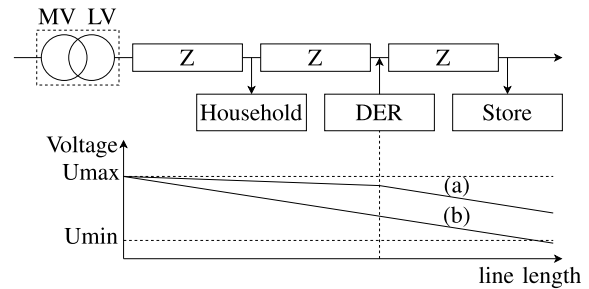


**FIGURE 2** Basic interpretation of distributed energy resource (DER) impact ( $Z$  = line impedance), (a) is with DER and has a positive impact, (b) is without DER and voltage drops below the limit at the end of the line

cause voltage deviations or by setting the frequency level so that the grid dynamics can be evaluated. The voltage as a function of the line length provides us insight on the impact of DERs. An active DER will cause a raised voltage near the POC. In Figure 2 this is shown as a positive effect while the voltage level stays within its boundaries for a longer line length. Issues will occur when multiple DERs are connected in an area where they can reinforce each other's behaviour. This may cause the maximum voltage level to be exceeded. To resolve this, DERs should implement functions to support the grid and change their output according to voltage and frequency levels [11, 25, 41].

Figure 3 depicts the simulation model in one block diagram. Again, colour codes are used to indicate the origin of the settings. The preset characteristics consist of the P(U), P(f), Q(P), and Q(U) blocks. The measurements are the output of the equivalent grid model (see Figure 4). The time constants are used as an input for the preset characteristics and can be changed according to DSO request. The user settings are simulation specific. On the one hand, a voltage and frequency error can be simulated to compensate for measuring issues. On the other hand, the minimum power factor can also be set. Needless to say, this will in real life be derived from the connection contract between DSO and the owner of the inverter.

### 3.2 | Equivalent grid model

The equivalent single-phase grid model, as illustrated in Figure 4, is used as a realistic representation of a grid. Since the voltage source block is ideal (this is the standard setting in Simulink) a source inductance is added to compensate for the short-circuit impedance of the second transformer winding. The line impedance is calculated based on the line length, with a resistance of  $0.38 \Omega$  per km and an inductance of  $0.72 \text{ mH}$  per km. While this model focuses on simulating voltage deviations by setting the source main voltage, only two main loads of  $9.2 \text{ kW}$  are used. A further segmentation of loads should be made when the mutual distance between households is of importance, and thus a line impedance between

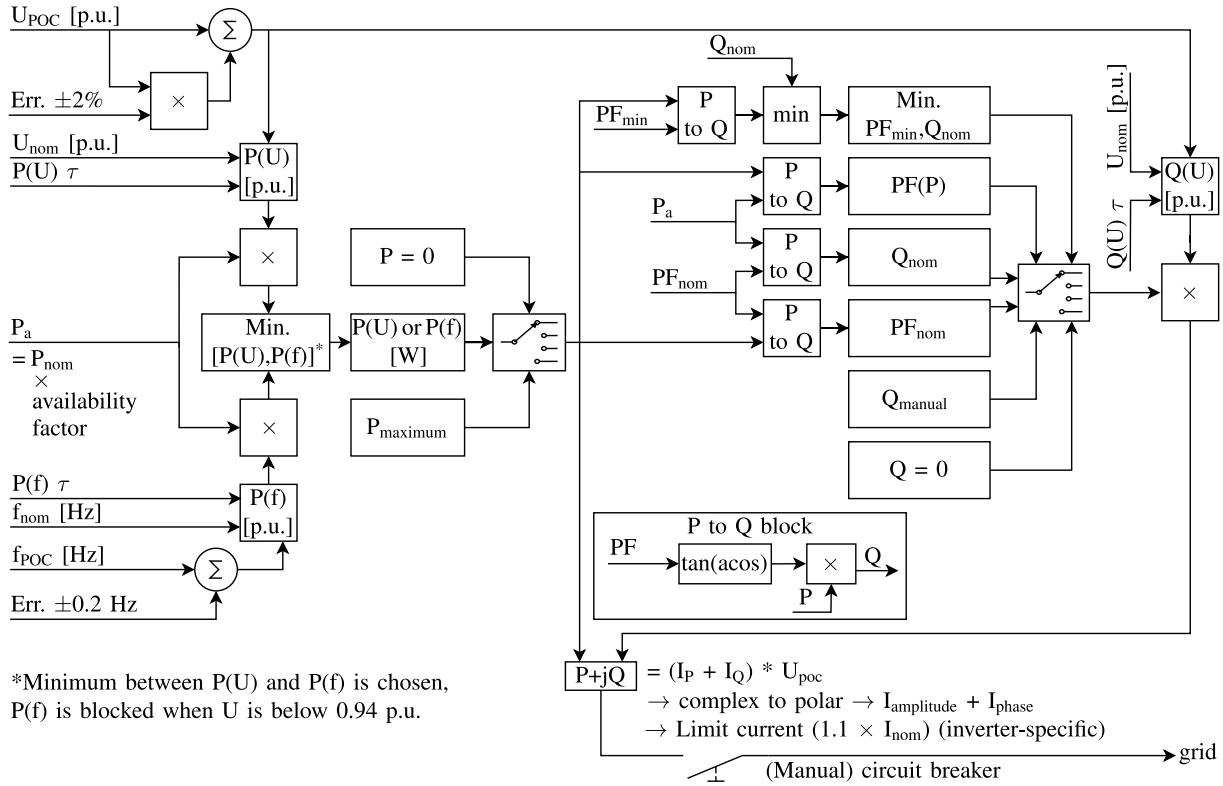


FIGURE 3 This flowchart represents the entire simulation model. All inputs, measurements and calculations are summarized in one block diagram

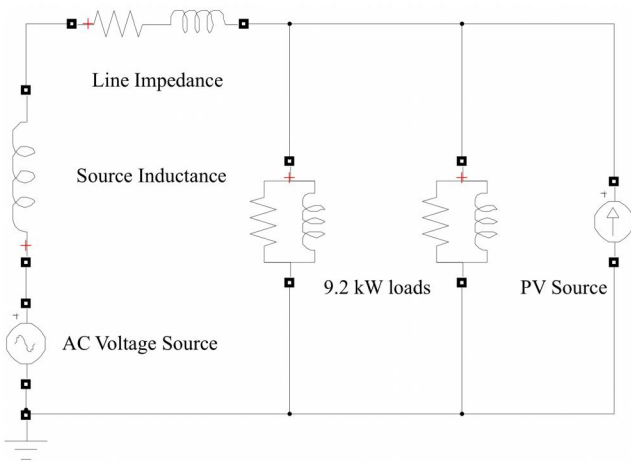


FIGURE 4 Equivalent single-phase grid model. A visual representation makes it straightforward to add or edit parameters

households should also be added. The aforementioned values for impedance and loads are always unique for a specific situation and should be changed accordingly when using this simulation model for other setups. The values for loads and PV sizes can be obtained by values given by the digital smart meter.

Simulink provides many useful standard blocks. Simple characteristics, such as P(U), Q(P), and Q(U) curves are implemented using 1-D lookup tables. The P(f) characteristic, implemented in layer 2, requires extra functionalities. More

complex functions are therefore implemented using a combination of 1-D lookup tables and MATLAB functions.

### 3.3 | Characteristics of control scheme

#### 3.3.1 | P(U) characteristic

It is necessary to calculate P(U) and Q(U) to calculate  $I_{amplitude}$  and  $i_{phase}$ . P is calculated by using a P(U) characteristic shown in Figure 5. The actual implementation is shown in Figure 6. The voltage [p.u.] values used for limiting P can differ according to DSO requirements.

While most regulations are based on p.u. values, this model also uses the voltage p.u. as an input for the P(U) characteristic. The implementation also requires a limit in output to prevent values lower than 0 and higher than 1. After this, the P(U) characteristic output is multiplied by the available P ( $P_{nominal}$  multiplied by an availability factor, depending on uncontrollable variables, e.g. sunlight). The availability factor can be used by the operator to limit the nominal power output caused by shadow, lack of sunlight, and so forth

#### 3.3.2 | P(f) characteristic

DERs can also have an impact on frequency levels. A single DER will not have a visual impact, but adding them all



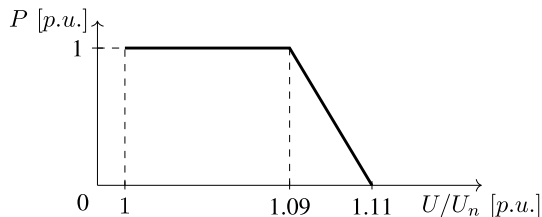


FIGURE 5 P(U) characteristic with a linear voltage limit from 1.09 p.u. to 1.11 p.u.

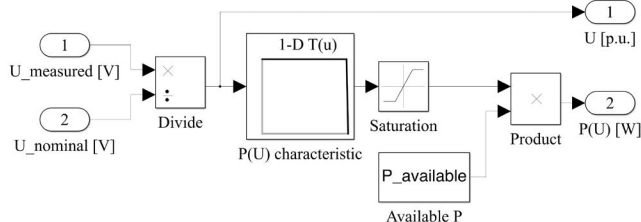


FIGURE 6 The method for implementing the P(U) characteristic in the model

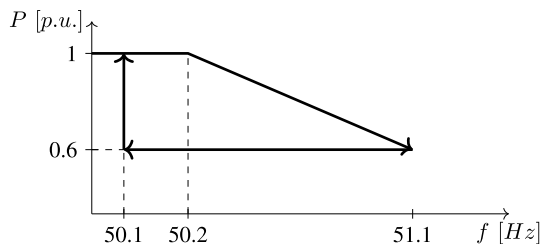


FIGURE 7 P(f) characteristic, proposed in [41, p. 29] and implemented in simulation model

together will. To compensate for this change in frequency level, the power output can be adapted if over- or under-frequency is present. The P(f) characteristic shown in Figure 7 is described in [41]. A value threshold is applied to maintain 0.6 p.u. P output when frequency reaches 51.1 Hz. To prevent frequency levels from rising too fast again when frequency drops (P output will also rise again), the P output is limited to 0.6 p.u. until the frequency drops below 50.1 Hz.

### 3.3.3 | Q(P) modes

The output of the P(U) or P(f) characteristic is used as an input for calculating Q(P). This can be calculated using different user-specific Q modes. The following paragraphs explain all the configured modes. In the simulation model, a switch selector determines which mode is currently preferred. The applicability of Q(P) modes is not further discussed, as this is beyond the scope of this paper. A specific case study with only changing the Q(P) mode could determine the most suitable mode.

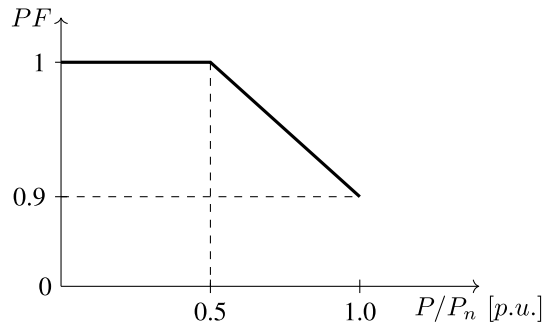


FIGURE 8 PF(P) characteristic indicating a decrease in PF when more than 0.5 P p.u. is delivered

#### Q(P) mode 1

The first Q-mode outputs the minimum value between  $Q_{nominal}$  and  $Q_{PFmin}$ . The minimum power factor (PF) in the model is 0.85 but can be changed by the operator. Note that the P input for both subsystems is different. For calculating  $Q_{nominal}$ , a limitation in Q is not taken into account (the limitation being the availability factor, depending on sunlight etc.).

#### Q(P) mode 2

The second mode uses a varying PF as a function of P output. Figure 8 illustrates that the PF varies from 0.9 to 1. The slope from 0.5 to 1.0 p.u. P can be changed according to DSO or local requirements.

#### Q(P) mode 3

The third mode uses  $PF_{nominal}$  to calculate the Q(P) output. In this mode, the Q output is always proportional to the P output.

#### Q(P) modes 4, 5, and 6

The remaining three modes are the following:

- $Q_{nominal}$  calculated with  $PF_{nominal}$  and  $P_{nominal}$
- constant Q,
- zero Q when no Q support is expected.

All six modes will have a different impact on voltage levels. The best mode will differ according to the situation and the general voltage profile of the feeder. Currently, the preferred mode is chosen manually to better evaluate the impact in specific situations. Selecting the Q-mode with the lowest reactive power output will be beneficial for the PV owner, but less beneficial for supporting voltage levels at the POC.

### 3.4 | Q(U) characteristic

The output of the Q-mode selector is used to calculate the actual Q output. This calculation is done using a Q(U) characteristic, shown in Figure 9.

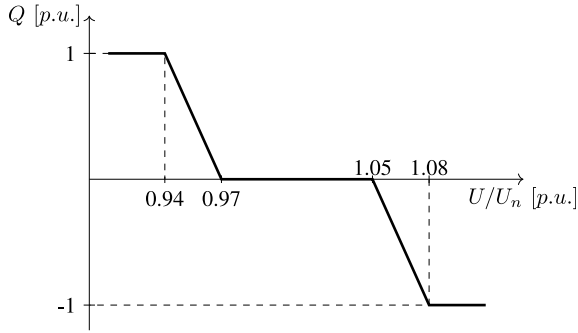


FIGURE 9 Q(U) characteristic with the deadband as discussed in 2.1.2

### 3.5 | Use of variable time constants in P(U), P(f), and Q(U) characteristics

In order to slow down the response of generating units, additional delay in the form of a first order low-pass filter is introduced. The P(U), P(f) and Q(U) characteristics use a different time constant. This time constant is changed manually, but in real life operation it is requested by the relevant DSO.

To offer more flexibility regarding time constants, the Model Discretizer (Simulink app) is used. A continuous time transfer function can be configured and is used to compute the discrete transfer function. The zero-order hold method is chosen, since this method uses the exact continuous value and holds it for (in this case) 0.02 s.

The possibility of changing the time constant, even during simulation, is interesting for comparing the impact of different time constants. Also, this can simulate the request of DSOs. As mentioned above, a specific time constant can be requested by the DSO to influence the impact of the DER. A smaller time constant will also bring more risk, as this can cause oscillations due to sudden changes of available P and Q.

## 4 | SIMULATION RESULTS

To validate the simulation model, random values for the voltage and frequency set points (see Table 1) are set to explain the output and indicate the accuracy of implementation. Table 1 summarizes the test conditions. A relatively large step size of 0.2 s is chosen to improve simulation time. However, larger system studies can be performed with respecting slow dynamics (in order of seconds). These are valid for both case studies. An R/X ratio of around 1 to 3 is usual in LV grids [5]. In this case, a ratio of around 2 is used. The reactance X depends on the inductance L and the frequency f. It is given by

$$X = \omega L \quad (5)$$

TABLE 1 Model settings used in the case studies

Description	Value or setting
Step size	0.02 s
PF <sub>nominal</sub>	0.90
PF <sub>minimum</sub>	0.85
Q-mode	Q-mode 1 (see 3.3.3)
P <sub>nominal</sub>	10.00 kW
P <sub>available</sub>	1.00 p.u.
P(U) $\tau$	0.40 s
P(f) $\tau$	0.40 s
Q(U) $\tau$	0.40 s
Main source voltage	414.00 V
Line length	1.00 km
Line resistance	0.38 $\Omega$ /km
Line inductance	0.72 mH/km
Two extra loads	Both off
Overvoltage set points	[1.00 1.05 1.09 1.10 1.11]
Undervoltage set points	[1.00 0.98 0.96 0.94 0.92]
Voltage error	0.00%
Overfrequency set points	[50.00 50.50 51.10 50.50 50.00 50.00]
Underfrequency set points	[50.00 49.80 49.50 49.00 50.00 50.00]
Frequency error	0.00 Hz

where

$$\omega = 2\pi f \quad (6)$$

### 4.1 | Case 1: undervoltage with overfrequency

Figure 10 depicts the P(f) characteristic and the overwriting of the P(U) characteristic when the voltage level is 0.94 p.u. or lower (see Figure 3). The overwrite is implemented to prevent a bigger voltage drop when both undervoltage and overfrequency are present at the same time. At  $t = 4.58$  s, the current limit is reached (see difference between calculated and measured P and Q output). This indicates one of the restrictions of the inverter. Note that this is also the best-case scenario with an available power of 100%, thus output power can even be more restricted. At 2.00 s, overfrequency occurs and P output drops according to P(f) characteristic (see Figure 7). At 4.04 s, voltage drops below the level, according to Figure 9, that activates the Q(U) characteristic. Voltage keeps dropping, and at 4.14 s, it reaches 0.94 p.u. and indicates an overwriting of the P(f) characteristic by the P(U) characteristic (see \* bottom left in Figure 3). Finally, at 4.58 s, a saturation in

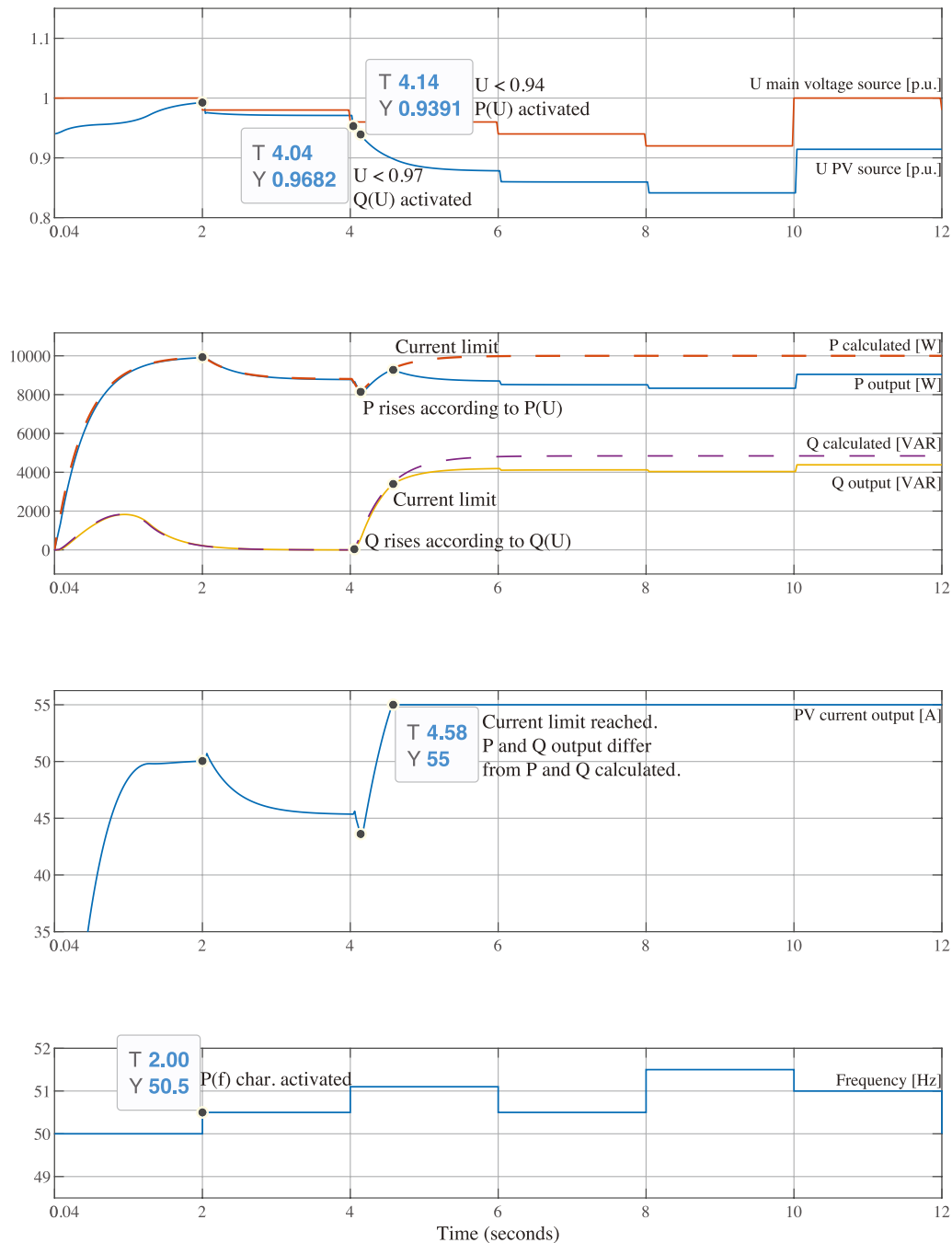


**FIGURE 10** Case 1: when both undervoltage and overfrequency occur, the interaction of the P(U) and P(f) characteristic can be denoted. The simulation parameters are set as defined in Table 1

the inverter occurs and current is limited. The second pane indicates this as a difference between the calculated and actual power output.

### 4.2 | Case 2: overvoltage with overfrequency

Figure 11 depicts the use of the minimum between P(U) and P(f) characteristics for voltage levels of 0.94 p.u. or higher. Starting from 4.04 s, the P(U) characteristic outputs less P and

is therefore determining the calculated P output. At 2.00 s, overfrequency occurs and P output drops according to P(f) characteristic (see Figure 7). At 4.04 s, the voltage exceeds 1.05 and activates the Q(U) characteristic (see Figure 9). Note that case 2 activates the opposite side of the characteristic than case 1. At 6.04 s and 8.04 s, voltage reaches 1.11 p.u., and P and Q drop accordingly to mitigate the voltage violation (see Figure 5). It also depicts the overwriting of the P(f) characteristic by the P(U) characteristic (see \* bottom left in Figure 3). Finally, at 10.06 s, voltage is between the limits—P



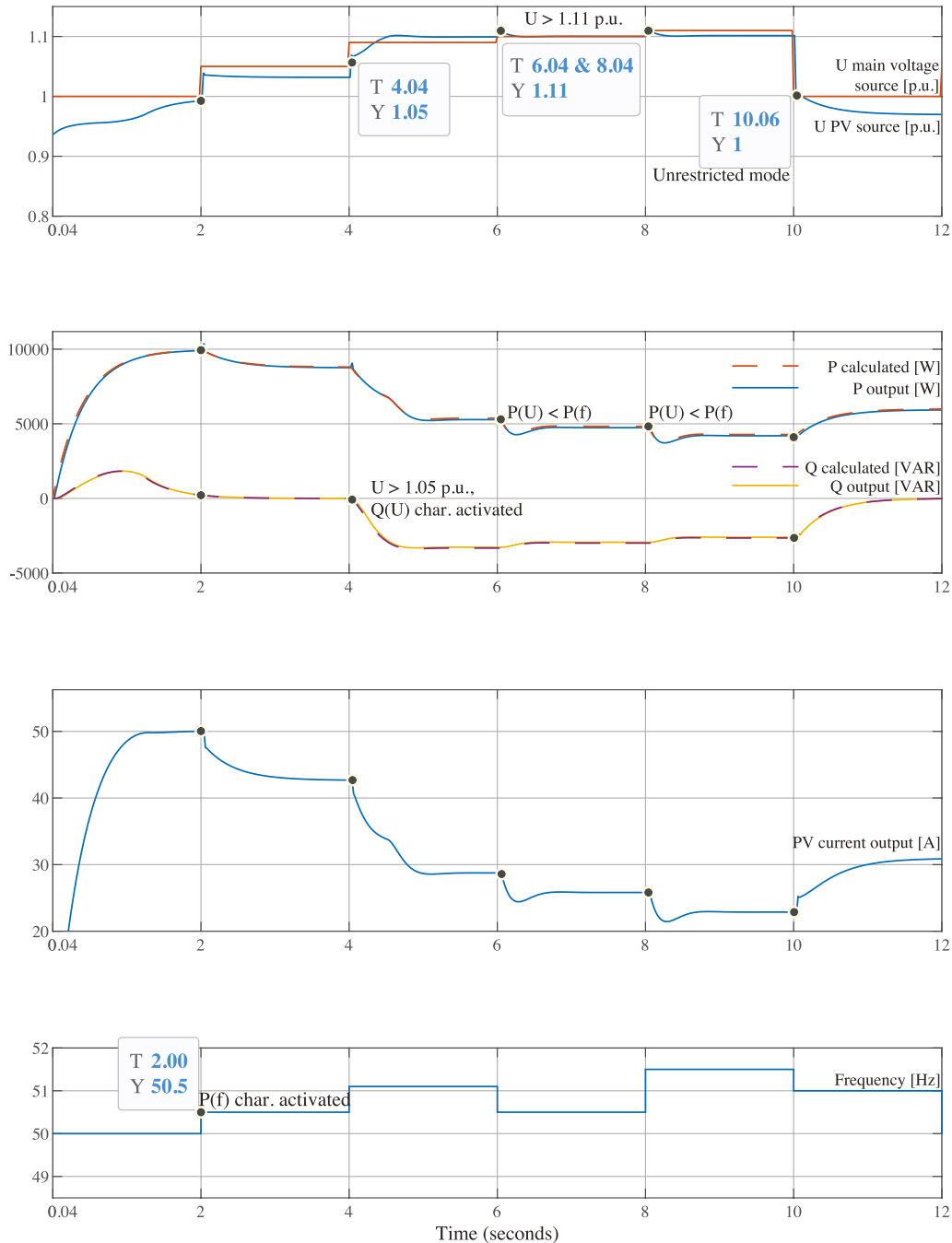


**FIGURE 11** Case 2: when both overvoltage and overfrequency occur, the minimum output between  $P(U)$  and  $P(f)$  is chosen.  $Q$  output is still controlled by the  $Q(U)$  characteristic. The simulation parameters are set as defined in Table 1

and  $Q$  outputs are unrestricted. This case is similar to overvoltage with overfrequency, as the  $P(f)$  characteristic is only active between 2.00 s and 4.04 s.

## 5 | CONCLUSIONS

This paper gives a brief overview of the voltage control methods on LV power grids. The most common support, active and reactive power compensation using inverters, is

further discussed. DSM is promising but requires smart appliances and household participation. Therefore, it currently is not a sufficient solution.

A literature study identifies the present issues that voltage control techniques are facing. Control parameters (such as the ability to choose a  $Q(P)$  mode) are often fixed, which does not allow adequate variation when the simulation model is used to determine the most appropriate solution for grid issues. The development in a visual simulation model such as Simulink is therefore recommended.

Two test cases were demonstrated to validate the model with (1) undervoltage with overfrequency and (2) overvoltage with overfrequency. However, the case studies are presented to validate the separate parameters of the model; therefore, they are kept rather simple. A set of new parameters for each case study would result in a more difficult validation of the implemented functionalities. Parameters not addressed in the two case studies, however, have been tested to guarantee correct implementation. The changes in the P and Q outputs were traced back to the implemented characteristics. The results are thus satisfactory.

The simulation model was developed to provide grid operators with a possibility to perform tests to predict the grid response. This way, further issues with connecting new DERs may be predicted. Figure 4 depicts a simplified version of a voltage source, loads, and a PV source. As this was a test case study, the schematic should be adjusted according to the values given by the digital smart meter to set the load sizes and PV sizes.

In future research, the impact of changing only the Q (P) mode parameter could be studied. This could result in better comprehension of the reactive power response of the grid and the role of the reactive power capacity of DERs.

## ORCID

Arjen Mentens  <https://orcid.org/0000-0002-2083-960X>

## REFERENCES

- Energy Statistics – An Overview. (2020). <https://ec.europa.eu/eurostat/statistics-explained/index.php?title=Energystatistics-anoverview&oldid=492784#Grossinlandenergyconsumption> (visited on 11/16/2020)
- Europe 2020 – Overview. <https://ec.europa.eu/eurostat/web/europe-2020.indicators> (visited on 11/16/2020)
- Masson, G., Kaizuka, I.: Trends in Photovoltaic Applications, IEA PVPS Technical Report (2019)
- Crăciun, B. et al.: Overview of recent grid codes for PV power integration. In: 2012 13th International Conference on Optimization of Electrical and Electronic Equipment, (OPTIM), pp. 959–965 (2012). <https://doi.org/10.1109/OPTIM.2012.6231767>
- Hes, S., Kula, J., Svec, J.: Increasing DER hosting capacity in LV grids in the Czech Republic in terms of European Project InterFlex. In: 2019 IEEE PES Innovative Smart Grid Technologies Europe, (ISGT Europe), pp. 1–5. (2019). <https://doi.org/10.1109/ISGT Europe.2019.8905664>
- Dierckxsens, C.: METAPV: Technical Project Overview and Results. 3E, Brussels (2015). [http://www.metapv.eu/sites/default/files/PRPR104282\\_FullProjectReportF.pdf](http://www.metapv.eu/sites/default/files/PRPR104282_FullProjectReportF.pdf)
- Collins, L., Ward, J.K.: Real and reactive power control of distributed pv inverters for overvoltage prevention and increased renewable generation hosting capacity. *Renew. Energy*. 81, 464–471 (Sep. 2015). <https://doi.org/10.1016/j.renene.2015.03.012>. ISSN: 18790682
- Tonkoski, R., Turcotte, D., El-Fouly, T.H.M.: Impact of high PV penetration on voltage profiles in residential neighborhoods. *IEEE Trans. Sustain. Energy*. 3(3), 518–527 (2012). <https://doi.org/10.1109/TSTE.2012.2191425>. ISSN: 19493029
- Vlaamse Regulator voor de Elektriciteits-en Gasmarkt: Energiemarkt in Vlaanderen en België - Marktmonitor (2020). [https://www.vreg.be/sites/default/files/document/rapp-2020-21.pdf\(visitedon01/05/2021](https://www.vreg.be/sites/default/files/document/rapp-2020-21.pdf(visitedon01/05/2021)
- Dexters, A.: Energiebeheersystemen: Voltage control [course]. Gezamenlijke opleiding Industriële Ingenieurswetenschappen UHasselt & KU Leuven, Diepenbeek, Belgium (2019)
- Commission regulation (EU) of 14 April 2016/631 establishing a network code on requirements for grid connection of generators. *Off. J. Eur. Union*. (2016)
- Honrubia-Escribano, A. et al.: Generic dynamic wind turbine models for power system stability analysis: a comprehensive review. *Renew. Sustain. Energy Rev.* 81, 1939–1952 (2018). <https://doi.org/10.1016/j.rser.2017.06.005>. [https://www.vreg.be/sites/default/files/document/rapp-2020-21.pdf\(visitedon01/05/2021](https://www.vreg.be/sites/default/files/document/rapp-2020-21.pdf(visitedon01/05/2021)
- Betancourt-Paulino, P. et al.: On the perspective of grid architecture model with high TSO-DSO interaction. *IET Energy Syst. Integr.* <https://doi.org/10.1049/esi2.12003>. ISSN: 2516-8401. [http://ietresearch.onlinelibrary.wiley.com/doi/abs/10.1049/esi2.12003\(visitedon03/04/2021\)](http://ietresearch.onlinelibrary.wiley.com/doi/abs/10.1049/esi2.12003(visitedon03/04/2021))
- Wankhede, S.K., Paliwal, P., Kirar, M.K.: Increasing penetration of DERs in smart grid framework: a state-of-the-art review on challenges, mitigation techniques and role of smart inverters. *J. Circuit Syst. Comp.* 29(16), 2030014 (2020). <https://doi.org/10.1142/S0218126620300147>. ISSN: 0218-1266
- Ustun, T.S., et al.: Optimal pv-inv capacity ratio for residential smart inverters operating under different control modes. *IEEE Access*. 8, 116078–116089 (2020). <https://doi.org/10.1109/ACCESS.2020.3003949>
- Gonzalez-Longatt, F.M., et al.: Power converters dominated power systems. In: *Modelling and Simulation of Power Electronic Converter Dominated Power Systems in Power Factory*, pp. 1–35.(2021). <https://doi.org/10.1007/978-3-030-54124-81>. <http://link.springer.com/443.webvpn.fjmu.edu.cn/chapter/10.1007/978-3-030-54124-81> (visited on 11/09/2020)
- Shabestary, M.M., Mohamed, Y.A.-R.I.: Autonomous coordinated control scheme for cooperative asymmetric low-voltage ride-through and grid support in active distribution networks with multiple dg units. *IEEE Trans. Smart Grid*. 11(3), 2125–2139 (2020). <https://doi.org/10.1109/TSG.2019.2948131>
- Bonfiglio, A. et al.: Optimal control and operation of grid-connected photovoltaic production units for voltage support in medium-voltage networks. *IEEE Trans. Sustain. Energy*. 5(1), 254–263 (2014). <https://doi.org/10.1109/TSTE.2013.2280811>
- Aristidou, P., Valverde, G., Van Cutsem, T.: Contribution of distribution network control to voltage stability: a case study. *IEEE Trans. Smart Grid*. 8(1), 106–116 (2017). <https://doi.org/10.1109/TSG.2015.2474815>
- Li, C. et al.: A hybrid control strategy to support voltage in industrial active distribution networks. *IEEE Trans. Power Deliv.* 33(6), 2590–2602 (2018). <https://doi.org/10.1109/TPWRD.2018.2863226>
- Mohamed, Y.A.-R.I., El-Saadany, E.F.: A control method of grid-connected PWM voltage source inverters to mitigate fast voltage disturbances. *IEEE Trans. Power Syst.* 24(1), 489–491 (2009). <https://doi.org/10.1109/TPWRS.2008.2006996>
- Maharjan, S., Khambadkone, A.M., Peng, J.C.-H.: Robust constrained model predictive voltage control in active distribution networks. *IEEE Trans. Sustain. Energy*. 12(1), 400–411 (2021). <https://doi.org/10.1109/TSTE.2020.3001115>
- Karagiannopoulos, S. et al.: Active distribution grids providing voltage support: the swiss case. *IEEE Trans. Smart Grid*. 12(1), 268–278 (2021). <https://doi.org/10.1109/TSG.2020.3010884>
- Joseph, A., Smedley, K., Mehraeen, S.: Secure high DER penetration power distribution via autonomously coordinated volt/VAR control. *IEEE Trans. Power Delivery*. 35(5), 2272–2284 (Oct. 2020). <https://doi.org/10.1109/TPWRD.2020.2965107>. ISSN: 0885-8977
- Yamashita, K.: Modelling of inverter-based generation for power system dynamic studies, CIGRE Joint Working Group Technical Report (2018).
- Al-Shetwi, A.Q., Sujod, M.Z., Blaabjerg, F.: Low voltage ride-through capability control for single-stage inverter-based grid-connected photovoltaic power plant. *Sol. Energy*. 159, 665–681 (2018). <https://doi.org/10.1016/j.solener.2017.11.027>
- Dugan, R., Sunderman, W., Seal, B.: Advanced inverter controls for distributed resources. In: 22nd International Conference and Exhibition on Electricity Distribution (CIGRE 2013), p. 1221. Institution of

- Engineering and Technology, Stockholm (2013). ISBN: 978-1-84919-732-8. <https://doi.org/10.1049/cp.2013.1126>
28. Sunderman, W., Dugan, R.C., Smith, J.: Open source modelling of advanced inverter functions for solar photovoltaic installations. In: 2014 IEEE PES T&D Conference and Exposition, Chicago, pp. 1–5.(2014). doi : <https://doi.org/10.1109/tde.2014.6863399>. ISBN: 9781479936557
  29. Seal, B., Ealey, B.: Common Functions for Smart Inverters, Technical Report, Electric Power Research Institute, Palo Alto, CA, pp. 1–170 (2016)
  30. Sarmiento, J.E., Carreno, E.M., Zambroni de Souza, A.C.: Modelling inverters with volt-var functions in grid-connected mode and droop control method in islanded mode. *Electr. Power Syst. Res.* 155, 265–273 (Feb. 2018). <https://doi.org/10.1016/j.epsr.2017.10.020>. ISSN: 03787796
  31. Famoso, F. et al.: Performance comparison between micro-inverter and string-inverter photovoltaic systems. *Energy Procedia.* 81, pp. 526–539 (2015). <https://doi.org/10.1016/j.egypro.2015.12.126>
  32. Chattopadhyay, S.K., Chakraborty, C.: Photovoltaic central inverters: performance evaluation and comparative assessment. In: Proceedings IECON 2017 – 43rd Annual Conference of the IEEE Industrial Electronics Society, vol. 2017, pp. 6419–6424. Institute of Electrical and Electronics Engineers Inc. (Dec. 2017). <https://doi.org/10.1109/IECON.2017.8217118>. ISBN: 9781538611272
  33. Harb, S. et al.: Microinverter and string inverter grid-connected photovoltaic system — a comprehensive study. In: 2013 IEEE 39th Photovoltaic Specialists Conference, (PVSC), pp. 2885–2890.(2013). <https://doi.org/10.1109/PVSC.2013.6745072>
  34. Nassif, A. B. et al.: Feeder voltage management through smart inverter advanced functions and battery energy storage system. In: IEEE Power and Energy Society General Meeting, vol. 2018-. IEEE Computer Society (Dec. 2018). ISBN: 9781538677032. <https://doi.org/10.1109/PESGM.2018.8586083>
  35. Huang, J., et al.: Photovoltaic single-phase grid-connected inverter based on voltage and reactive power support. *IOP Conf. Ser. Mater. Sci. Eng.* 366, 012014 (2018). <https://doi.org/10.1088/1757-899X/366/1/012014>
  36. Zhao, X. et al.: Power system support functions provided by smart inverters – a review. *CPSS Trans. Power Electron. Appl.* 3(1), 25–35 (2018). <https://doi.org/10.24295/CPSSITPEA.2018.00003>
  37. Mirez, J.L. et al.: Energy management of distributed resources in microgrids. In: 2014 IEEE 5th Colombian Workshop on Circuits and Systems (CWCAS), pp. 1–5.(2014). <https://doi.org/10.1109/CWCAS.2014.6994607>
  38. Belmans, R.: Linear, Demand Response for Families, Technical Report. EnergyVille, Genk, Belgium (2014)
  39. Gottwalt, S. et al.: Demand side management-A simulation of household behaviour under variable prices. *Energy Pol.* 39(12), 8163–8174 (2011). <https://doi.org/10.1016/j.enpol.2011.10.016>
  40. CREG: Strategische Reserve. <https://www.creg.be/nl/professionals/marktwerking-en-monitoring/strategische-reserve>. Accessed 13 April 2020
  41. CENELEC: EN 50549-2:2018 Requirements for generating plants to be connected in parallel with distribution networks - Part 2: Connection to a MV distribution network - Generating plants up to and including Type B. (2018)

**How to cite this article:** Mentens, A., et al.: Impact of advanced inverter functions on low-voltage power grids. *IET Energy Syst. Integr.* 3(4), 426–436 (2021). <https://doi.org/10.1049/esi2.12018>